접착 및 계면 제18권 제3호, 2017년
〈연구논문(Original Article)〉

Journal of Adhesion and Interface Vol.18, No.3, 2017
http://dx.doi.org/10.17702/jai.2017.18.3.109

PVK-*b*-PVP 블록 공중합체의 존재 하에서 안정한 비 수계 그래핀 분산액을 위한 용매-고분자 상호작용에 관한 연구

박경태 · Suguna Perumal · 이향무 · 김영현 · 정인우†

경북대학교 공과대학 응용화학과

(2017년 7월 21일 접수, 2017년 8월 29일 수정, 2017년 9월 4일 채택)

Solvent-Polymer Interactions for Stable Non-Aqueous Graphene Dispersions in the Presence of PVK-*b*-PVP Block Copolymer

Kyung Tae Park · Suguna Perumal, Hyang Moo Lee, Young Hyun Kim and In Woo Cheong†

Department of Applied Chemistry, School of Engineering, Kyungpook National University, Buk-gu, Daehak-ro 80, Daegu 41566, South Korea

(Received July 21, 2017; Revised August 29, 2017; Accepted September 4, 2017)

요 약 : 본 연구에서는 poly(*N*-vinyl carbazole) (PVK), poly(4-vinylpyridine) (PVP), PVK-*b*-PVP 블록 공중합체를 RAFT 중합법으로 합성하였으며, 이를 이용하여 ethanol, *N*-methyl-2-pyrrolidone (NMP), dichloromethane (DCM), tetrahydrofuran (THF)와 같은 비 수계 용매에서 그래핀 분산액을 제조하였다. 합성된 고분자의 화학적 구조는 양성자 및 탄소 핵자기 공명 분광기(^{1}H-, ^{13}C-NMR), 크기 배제 크로마토그래피 (size exclusive chromatography, SEC), 시차 주사 열량계 (differential scanning calorimetry, DSC)를 이용하여 분석하였으며, 그래핀 분산액의 분산 안정성은 Turbiscan을 이용하여 시간에 따른 터비스캔 안정성 지수(Turbiscan stability index, TSI)를 측정, 정량적으로 평가하였다. 용매, 고분자, 그래핀의 표면장력(σ), 용해도 상수(δ)를 이용하여 물질간의 상호작용에 대하여 설명하였으며, 이를 바탕으로 용매와 그래핀간의 용해도와 표면장력의 차이가 분산안정성에 큰 영향을 미침을 확인하였다. 그래핀의 분산 안정성이 좋지 못한 ethanol 및 THF 용매 하에서 PVK-*b*-PVP를 사용하여 그래핀을 분산시킬 경우 낮은 TSI값을 효과적으로 유지할 수 있었으며, 그래핀을 잘 분산시킨다고 알려진 NMP에 비하여 DCM이 더 좋은 그래핀 분산안정성을 보임을 확인하였다.

Abstract: Poly(N-vinyl carbazole) (PVK) homopolymer, poly(4-vinylpyridine) (PVP) homopolymer, and PVK-*b*-PVP block copolymer were synthesized by reversible addition-fragmentation chain transfer (RAFT) polymerization and the polymers were used to prepare non-aqueous graphene dispersions with four different solvents, ethanol, N-methyl-2-pyrrolidone (NMP), dichloromethane (DCM), and tetrahydrofuran (THF). ^{1}H- and ^{13}C-NMR spectroscopy, size exclusion chromatography (SEC), and differential scanning calorimetry (DSC) were carried out to confirm the chemical structure of the polymers. Stability of graphene dispersions was measured by on-line turbidity measurement. Time-dependent Turbiscan Stability Index (TSI) values were interpreted in terms of surface tension (σ) and solubility parameter (δ) among solvents, polymers, and graphene. It was confirmed that the solubilities of polymer and surface tension between solvent and graphene affected the dispersion stability of graphene. PVK-*b*-PVP block copolymer could effectively maintain the low TSI values of graphene dispersions in ethanol and THF, which have been known as poor solvents for graphene dispersions. It can also be noted that DCM shows good dispersion stability comparable to NMP, which has been known as the best solvent for graphene dispersion.

Keywords: *Graphene, Non-aqueous Dispersion, Block copolymer, Solvent-polymer Interactions*

† Corresponding author: In Woo Cheong (inwoo@knu.ac.kr)

1. Introduction

Graphene is one of the most attractive materials in these days due to its unique mechanical, chemical, electrical, and thermal properties [1-4]. Due to these distinctive properties of graphene, it has been introduced in applications, such as nanoelectronics, transistor, memory device, transparent screen, sensor, hydrogen storage, and biomedical technology [5-10].

For the applications of graphene, several methods producing single- or few-layer graphenes have been developed and studied, e.g., SiC epitaxial growth, chemical vapor deposition, mechanical peeling, and liquid-phase exfoliation so on.[11,12,2] Among these, liquid-phase exfoliation has emerged for mass production of graphene with low cost. Sonication-assisted liquid-phase exfoliation of graphene by surfactant or solvent has been extensively studied due to minimal defects, which cannot be achieved in chemical functionalization including oxidation and reduction [13-15].

Graphene can be prepared by surfactant-free exfoliation of graphite via chemical wet dispersion, followed by ultrasonication in organic solvents [16]. Organic solvents which have similar surface tensions with graphite (e.g., NMP or DMF) seem to be suitable to minimize the interfacial tension between the liquid and graphene nanoplatelets [17]. However, a high boiling point limits process efficiency in real manipulation, particularly in organic electronics. In order to produce graphene by liquid phase exfoliation in low boiling solvents, several attempts have done like solvothermal-assisted exfoliation process of expanded graphite in a highly polar organic solvent and dispersion of graphene in ethanol using a solvent exchange method [18,19]. Extensive studies have been done to exfoliate graphite into graphene with small organic molecules and conventional or synthesized polymers as surfactants in water or in organic solvents with low boiling points [20-22]. On the other hand, the yield of single-layer graphene platelets is relatively low or long sonication time is required. The surfactants used also can decrease the electrical property of graphene.

To address this issue, our group have designed and developed block copolymer dispersants for graphene dispersions based on the knowledge of adhesion forces between the basal surface of graphene and substituents of various monomers [23-26]. Our approach has mainly been focusing on the graphene-philic blocks; however, solvent-graphene and solvent-lyophilic block interactions should be considered as critical factors determining the dispersion stability of graphene. To the best of our knowledge, there are a few works on the details of the interactions between solvent-polymer or solvent-graphene for stable graphene dispersion [27,28]. It is expected that fundamental understanding of the polymer- solvent or polymer-graphene systems will be of great help in expanding the applications of graphene as well as producing stable non-oxidized graphene dispersion with high concentrations.

In this study, poly(*N*-vinyl carbazole) (PVK) and poly(4-vinylpyridine) (PVP) were synthesized by reversible addition fragmentation chain transfer (RAFT) polymerization. Synthesized PVK was used as a macro chain transfer agent (PVK-TTC) to synthesize block copolymer of PVK-*b*-PVP by RAFT polymerization. Solvent-polymer interaction was studied by solubility tests in four different solvents, such as ethanol, NMP, DCM, and THF. The prepared homopolymers and block copolymer were used as dispersants for non-aqueous dispersion of graphene platelets, and their dispersion stability was investigated and compared by using on-line turbidity. Surface tension and solubility parameters between solvent-polymer and solvent-graphene were considered to explain the dispersion stability of graphene in different solvent-polymer pairs.

2. Experimental

2.1. Materials

VP monomer (95%, Aldrich, USA) was used after purification by an inhibitor remover column (inhibitor removers, Aldrich, USA). VK monomer (98%, TCI, Japan) was used as received without further purification. 2-(Dodecylthiocarbonothioylthio)-2-methylpropionic acid (TTC, 98%, Aldrich, USA), 1,4-dioxane (99.5%, Acros, USA), *N,N*-dimethyl formamide (DMF, 99.5%, Duksan, Korea), hexanes (95%, Duksan, Korea), THF (99.5%, Duksan, Korea), DCM (99.5%, Duksan, Korea), NMP (99.5%, Samchun, Korea), and ethanol (99.8%, Duksan, Korea) were used as received without further purification. 2,2'-Azobisisobutyronitrile (AIBN, 98%, Junsei, Japan) was used after recrystallization in methanol. Non-oxidative graphene (M-25, Graphene Nanoplatelets, XG Sciences, USA) was used as a graphene platelets source.

2.2. Syntheses of PVK-TTC, PVP-TTC, and PVK-b-PVP

PVK-*b*-PVP diblock copolymer was synthesized by stepwise RAFT polymerizations of VK and VP monomers in sequence. To synthesize PVK-TTC, VK (1.200 g, 6.210 mmol), TTC (0.023 g, 0.062 mmol), and AIBN (5.099 mg, 0.031 mmol) with 100:1:0.5 molar ratios were added with 1,4-dioxane (2.4 mL) into a 5 mL dry glass ampule equipped with a magnetic stirring bar, and then the solution was degassed by three freeze-pump-thaw cycles. The ampule was then flame-sealed under vacuum after purging with N_2, immersed into a preheated oil bath at 70 °C, and stirred for 24 h. The product was purified by precipitation in hexane three times. For PVP-TTC, VP monomer was used instead of VK and followed the same procedure mentioned previously. The prepared PVK-TTC was used as a macro-RAFT agent in the synthesis of PVK-*b*-PVP diblock copolymer. VP (0.394 g, 3.75 mmol), PVK-TTC (0.353 g, 0.03 mmol), and AIBN (0.49 mg, 0.003 mmol) with 125:1:0.1 molar ratios were added with 1,4-dioxane (1.5 mL) into a dry glass ampule equipped with a magnetic stirring bar, and then the procedures were performed as mentioned before. The resulting diblock copolymer was characterized by ^{1}H-NMR, ^{13}C-NMR, and DSC. The reaction schemes for PVK-TTC and PVK-*b*-PVP are shown in **Scheme 1**. Hereinafter, PVK-TTC and PVP-TTC are simply referred to as PVK and PVP, respectively.

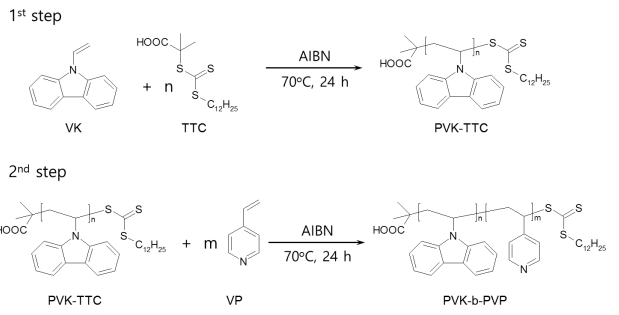

Scheme 1. Synthetic schemes of PVK-TTC homopolymers, and PVK-*b*-PVP diblock copolymer. For the preparation of PVP-TTC, predetermined amount of VP monomer was used instead of VK and followed the same procedure.

2.3. Preparation of graphene dispersions

For a study on dispersion stability of graphene platelets, non-oxidative graphene was dispersed with or without PVK-*b*-PVP diblock copolymer. In order to study the effect of homopolymer on the dispersion stability of graphene, PVK and PVP were also used and compared. Four different solvents, ethanol, NMP, DCM, and THF were used as dispersion media and the dispersion stability of graphene in different solvent was analyzed and compared. For the graphene dispersion, 20 mg of M-25, and 10 mg of homopolymer or block copolymer in 4 mL of solvent were added into a vial. The vial was then sonicated in a 40 kHz bath type sonicator (SD 80H, 50 W, S-D Ultra Sonic Cleaner, Korea) for 2 h. Ice was replenished every 30 minutes to maintain the temperature in the sonication bath. Right after the sonication, dispersion stability was measured using on-line turbidity as a functional of time for 24 h.

2.4. Characterization

^{1}H-NMR and ^{13}C-NMR spectra of PVK, PVP, and PVK-*b*-PVP were collected on a 500 MHz NMR spectrometer (AVANCE III 500, Bruker, Germany) in chloroform-*d* ($CDCl_3$, with 0.05% TMS, Aldrich, USA). The number-average molecular weight (M_n) and dispersity ($Đ_M$) of PVK were measured by size exclusion chromatography (SEC, Alliance e2695, Waters, USA) equipped with three different columns (Styragel HR3, Styragel HR4, and Styragel HR5E; Waters) in series. THF was used as an eluent (35 °C, 1 mL · min^{-1}). Polystyrene narrow standards (1,060 and 3,580,000 g · mol^{-1}, waters, USA; 1,320-2,580,000 g · mol^{-1}, Shodex, Japan) were used for calibration. For PVP, SEC system (P-4000, AT-4000, RI-101, Futecs, Korea) was used in DMF (KD-803's; Shodex, Japan) with 1 mL · min^{-1} at 40 °C. Poly(ethylene glycol) narrow standards (1,400-69,100 g · mol^{-1}, PSS GmBH, Germany) were used for calibration. The M_n of PVK-*b*-PVP was calculated from the ^{1}H-NMR data of PVK-*b*-PVP and the SEC data of PVK because PVP and PVK have different solubility. Glass transition temperature (T_g) of PVK-*b*-PVP was confirmed by differential scanning calorimetry (Q20, TA instruments, USA) with a temperature range from 80 to 280 °C and the heating rate of 10 °C · min^{-1}.

For the solubility tests, 10 mg of polymer was dissolved in 4 mL of solvent by gentle stirring or bath sonication (SD 80H) for 2 h at room temperature. The solubility of polymers was analyzed by optical turbidity

of transmittance and did not analyzed quantitatively.

In order to compare the stability of graphene dispersions of PVP, PVK, and PVK-*b*-PVP, 20 mg of M-25 in 4 mL of solvents was mixed with 10 mg of each polymer, and then sonicated for 2 h. For dispersion stability analyses, time-evolution back scattering data were measured by on-line turbidity (Turbiscan LAB, Formulaction Co., L'Union, France) at ambient conditions. From the back scattering data, the Turbiscan Stability Index (TSI) in the pre-defined zone (middle) of the sample vial bottle versus ageing time was obtained using the following equation:

$$TSI = \sum_i \frac{\sum_h \left| scan_i(h) - scan_{i-1}(h) \right|}{H} \quad (1)$$

where H is the length of the sample vial, h is the height of the measuring point, and $scan_i$ and $scan_{i-1}$ are Turbiscan intensities at measured time points. If the dispersion becomes unstable, the Turbiscan intensity difference becomes large, leading to an increase in the TSI value. Therefore, aggregation, precipitation, or creaming of the dispersion can be detected based on the TSI value.

3. Results and Discussion

3.1. PVP, PVK homopolymers, and PVK-b-PVP diblock copolymer

Structure of PVP and PVK homopolymers was confirmed by ^{1}H-NMR and shown in Figure 1(a) and Figure 1(b), respectively. As shown in Figure 1(a), the proton peaks from pyridine group were observed at 8.3 and 6.4 ppm. The proton peaks at the S-C<u>H$_2$</u>-C in TTC seems very weak but found around 3.2 ppm (refer to the inset), and the other proton peaks in TTC were observed at 0.5-1.0 ppm [29]. Further, ^{13}C-NMR was performed to confirm the chemical structure of PVP and the assignments were described (the spectra were omitted): the carbon peaks of pyridine were found at 152.2 (*1*, VP), 150.2 (unassigned, between *2* and *4* in pyridine unit, refer to the structure in Figure 1(a)), and 122.7 (*2*, VP). The M_n and $Đ_M$ of PVP were determined by SEC analyses ($M_{n,\ PVP}$ = 10.9 kg · mol^{-1} in DMF, $Đ_M$ = 1.1).

In Figure 1(b), the chemical shifts for the aromatic ring of VK were assigned [30]. The *f* peak was overlapped with the peak of S-C<u>H$_2$</u>-C from TTC at 3.2-2.5 ppm.

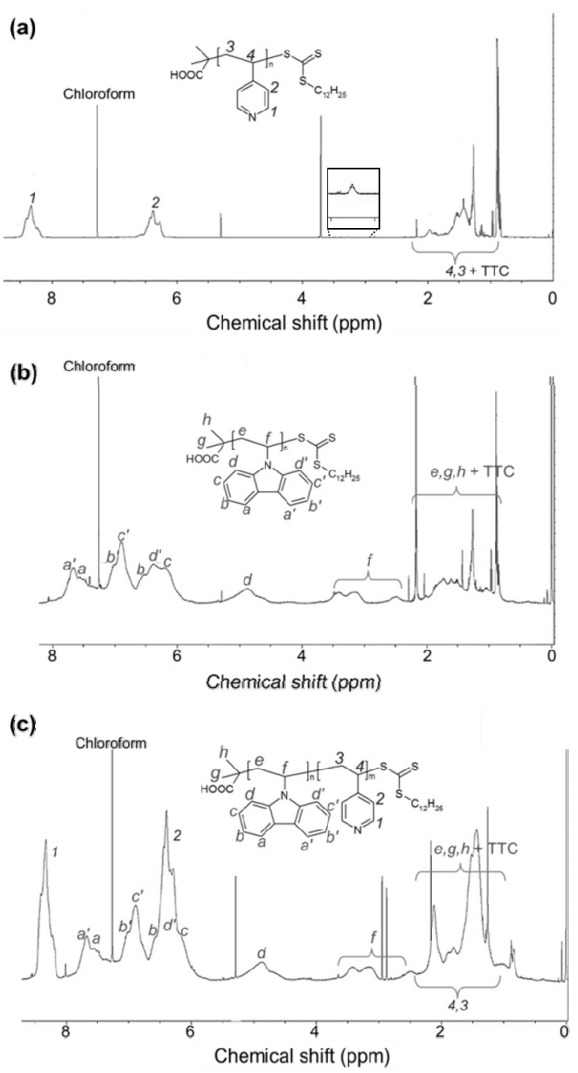

Figure 1. ^{1}H-NMR spectra for (a) PVP-TTC, (b) PVK-TTC, and (b) PVK-*b*-PVP diblock copolymer.

^{13}C-NMR also confirmed the chemical structure of PVK: δ 140.0, 137.5, 125.0 (*c*,*c*'), 123.8, 121.9, 120.2 (*a*'), 118.7 (*a*,*b*,*b*'), 110.3 (*d*'), and 108.1 ppm (*d*). The chemical shifts for <u>C</u>-N-<u>C</u> were observed at 140.0 and 137.5 ppm, respectively. The other unassigned carbons of carbazole group were observed at 123.8 and 121.9 ppm [30]. M_n and $Đ_M$ of PVK macro-RAFT agent were obtained by SEC analyses ($M_{n,\ PVK}$ = 11.7 kg · mol^{-1} in THF, $Đ_M$ = 1.4). The $Đ_M$ values of PVP and PVK indicate that the RAFT polymerization of PVK would be successful although they seem relatively high as compared with usual $Đ_M$ ranges of controlled living polymerizations.

The ^{1}H-NMR spectra of PVK-*b*-PVP diblock copolymer are shown in Figure 1(c). Proton peaks from

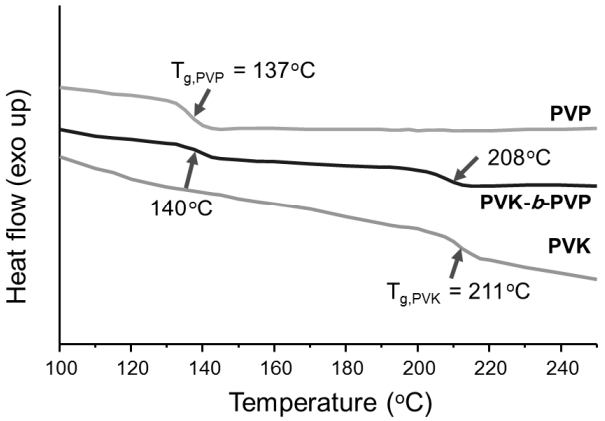

Figure 2. DSC curves for PVP, PVK-b-PVP, and PVK.

carbazole group were clearly observed except the overlapped peak of *d'* at 6.2-6.5 ppm. Proton peaks from pyridine group were observed at 8.3 and 6.4 ppm. ^{13}C-NMR was also performed to confirm the chemical structure of PVK-*b*-PVP and the carbon peaks of pyridine were found at 152.3, 150.2, and 122.7 ppm with pre-existing peaks from carbazole group. Due to the solubility problem of PVP block in THF, the M_n of PVK-*b*-PVP was estimated from the proton peak area ratio of VK (*a*+*a'*) to VP (*1*) peaks in the ^{1}H-NMR spectra ($M_{n,\ PVK\text{-}b\text{-}PVP}$ = 20.7 kg · mol^{-1}).

To confirm the block copolymer structure further, DSC analyses were carried out for PVP, PVK, and PVK-*b*-PVP, and the results are shown in Figure 2. Glass transition temperatures (T_gs) of the PVK and PVP blocks

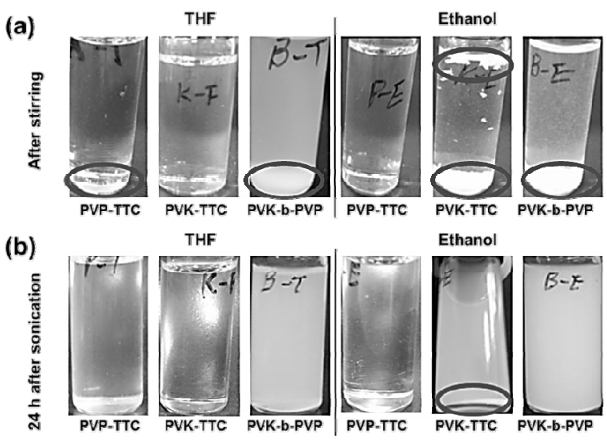

Figure 3. Photographic images of polymer solutions with PVP-TTC, PVK-TTC homopolymers, and PVK-*b*-PVP diblock copolymer prepared by (a) gentle stirring and (b) 24 h after sonication for 2 h. The red ovals indicate aggregates or precipitates of polymer.

in PVK-*b*-PVP were clearly observed at 208 °C and 140 °C, respectively. The T_g of PVP was 137 °C, and which was shifted to 140 °C in PVK-*b*-PVP. The T_g of PVK was 211 °C, and which was also shifted to 208 °C. The distinct T_g and their shifts of each block confirmed the formation of PVK-*b*-PVP.

3.2. Solubility of PVP, PVK, and PVK-b-PVP

Heterogeneous systems, such as dispersion, emulsion, and suspension can be kinetically stabilized in the presence of surfactants or dispersants. In order to disperse lyophobic materials, dispersants or dispersing agents would meet the criteria for amphiphilicity, i.e., one should be lyophilic and the other should be lyophobic [31-33]. From the previous work on force-distance analyses in AFM, it was found that pyridine group showed relatively higher adhesion force with the basal surface of non-oxidative graphene surface. The adhesion force values were found to be 9.3 nN and 5.5 nN for VP and VK, respectively [24]. Therefore, it can be suggested that PVP block is graphene-philic block and PVK block is lyophilic, respectively. However, solvent-solubility of PVK or PVP can also affect the dispersion stability of graphene, thus the solvent-solubility of homopolymers and diblock copolymer was studied with four different solvents. All three polymers were clearly dissolved in both NMP and DCM, and NMP has been known as a good solvent for graphene dispersions [17]. It was confirmed that PVP was dissolved well in ethanol but insoluble in THF. PVK was also dissolved completely in THF but insoluble in ethanol. PVK-*b*-PVP was not soluble in either ethanol or THF even after sonication. The photographic images of the polymer solutions in these two solvents are shown in Figure 3. As shown in Figure 3(a), both PVP in THF and PVK in ethanol were insoluble after gentle magnetic stirring and a large portion of insoluble precipitates were left, which were as highlighted as red ovals. Due to the partial affinity of PVK-*b*-PVP toward solvents, both THF and ethanolic solutions containing PVK-*b*-PVP show precipitates as well as turbidity.

In Figure 3(b), polymer solutions prepared by using sonication are shown. In the case of sonication, amounts of the precipitates were significantly reduced, but the solutions still remained as turbid. For PVP-TTC in THF, the solution prepared by using sonication has no precipitate but less clear when compared with PVP-TTC in THF prepared by using gentle magnetic stirring. This

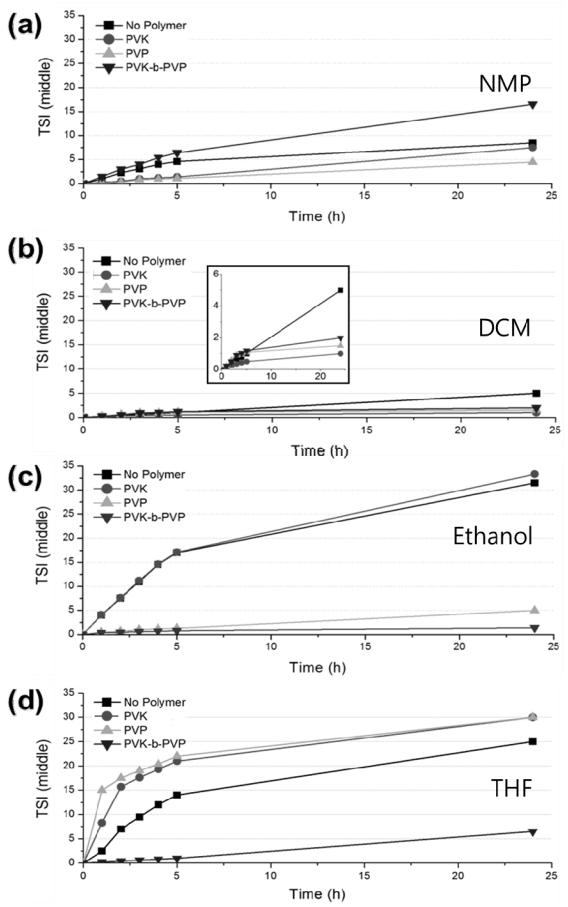

Figure 4. Time-dependent TSI values of graphene (M-25) dispersions with PVP, PVK, PVK-*b*-PVP, or without polymers in (a) NMP, (b) DCM, (c) ethanol, and (d) THF. The inset of (b) describes detailed TSI value variations with a magnified y-axis scale.

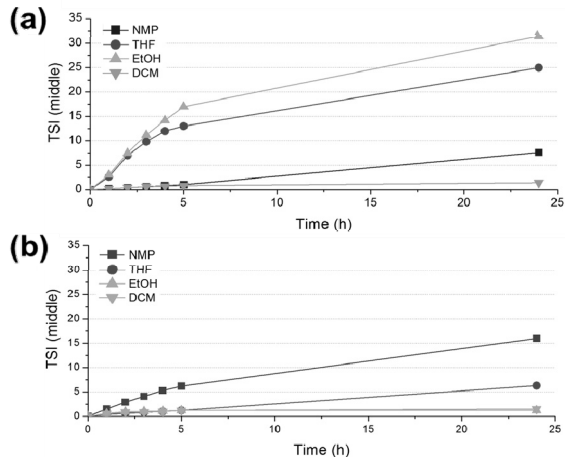

Figure 5. Time-dependent TSI values of graphene dispersions with different solvents: (a) without PVK-*b*-PVP and (b) with PVK-*b*-PVP diblock copolymer.

tendency was similarly observed in ethanolic solution containing PVK-TTC. For PVK-*b*-PVP solutions with 2h sonication, both THF and ethanol solutions were turbid without any precipitates, which indicates that PVK-*b*-PVP block copolymers self-assemble to micelles in both THF and ethanol.

These results were explained by solubility parameter (δ). For a polymer to dissolve spontaneously, ΔG_{mix} should be negative ($\Delta G_{mix} = \Delta H_{mix} - T\Delta S_{mix}$) and ΔH_{mix} must be small [34], and which can be expressed as below:

$$\Delta H_{mix} = V_{mix} (\delta_1 - \delta_2)^2 \phi_1 \phi_2 \quad (2)$$

where V_{mix} is the total volume of the mixture and ϕ is the volume fraction, respectively. Therefore, $(d_1 - d_2)^2$ goes to the minimum when $d_1 = d_2$, and in which solubility can be governed solely by entropy effects. Prediction of solubility is therefore based on finding solvents and polymers with similar solubility parameters. The d of PVK was reported as 20.1 $MPa^{1/2}$ [35] and that of PVP is known as 23.0 $MPa^{1/2}$ [36]. For solvents, the ds of ethanol, NMP, DCM, and THF were reported as 26.5, 22.9, 20.3, and 19.4 $MPa^{1/2}$, respectively [37]. Considering the difference $(d_1 - d_2)$, the d value of PVP is close to ethanol and NMP, while the d of PVK is close to DCM and THF.

3.3. Stability of graphene dispersions with PVK, PVP, and PVK-b-PVK

Time-evolution TSI values of the graphene dispersions in four different solvents were measured using Turbiscan and summarized in Figure 4. As expected, NMP shows good graphene dispersion stability with low TSI values as compared with the TSI values of the dispersions in ethanol and THF (Figure 4(a)). Interestingly, DCM also shows lower TSI values for all samples than the TSI values of the dispersions in NMP, and which reveals that DCM is a better solvent than NMP for dispersing graphene (Figure 4(b)). The surface tension (σ) of NMP is known as 40 $mN \cdot m^{-1}$ [17], and which is almost the same as that of graphene [16]. This may affect the dispersion stability of graphene since the solvent system can minimize the interfacial tension between exfoliated graphene surface and the surrounding medium. However, graphene dispersion without polymer in DCM shows lower TSI value than NMP as shown in Figure 4(b),

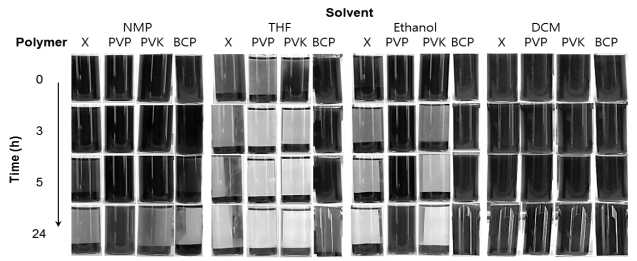

Figure 6. Photographic images of graphene dispersions in four different solvents with or without polymers. X and BCP indicate 'without polymer' and 'PVK-*b*-PVP block copolymer', respectively.

although the σ of DCM is 27 mN · m^{-1}. These results can be rationalized by solubility parameters, δ. The δ of graphene was estimated as 21 MPa$^{1/2}$ from Hansen solubility parameters [38]. As mentioned before, the order of the δs of solvents is as follows: ethanol (26.5 MPa$^{1/2}$) > NMP (22.9 MPa$^{1/2}$) > DCM (20.3 MPa$^{1/2}$) > THF (19.4 MPa$^{1/2}$). Therefore, DCM can be good solvent for graphene in terms of solubility parameter along with NMP. Thus, the results of dispersion stability in the presence of polymers can also be explained clearly by solubility parameter.

The σs of ethanol and THF are 22 mN · m^{-1} and 26 mN · m^{-1}, respectively; therefore, one can expect that the TSI values in ethanol and THF would be higher than those of NMP. The δ of PVK is 20.1 MPa$^{1/2}$, and which is in between DCM and THF; PVP is 23.0 MPa$^{1/2}$, which lies in between EtOH and NMP. Therefore, the ethanolic graphene dispersion with PVK shows poor stability like pristine graphene dispersion as shown in Figure 4(c). Likewise, the graphene dispersion in THF with PVP also shows poor stability, as shown in Figure 4(d). Among all the polymers, PVK-*b*-PVP block copolymer shows less TSI values and better dispersion stability in the poor solvents, ethanol and THF. In the cases of good solvents, NMP and DCM, higher TSI values are observed in PVK-*b*-PVP.

Time-dependent TSI values of graphene dispersions with different solvents were summarized in Figure 5. As shown in Figure 5(a), the dispersion stability of graphene without polymers can be listed in the following order: DCM > NMP >> THF > ethanol. The dispersion stability of the pristine graphene in various solvents can be easily interpreted in terms of δ rather than interpreted in terms o. The interpreted in terms o of NMP is the same as that of graphene (40 mN · m^{-1}), but it differs by ~13 compared to DCM (27 mN · m^{-1}). From the aspect of the solubility parameter, however, it can be seen that δ (21 MPa$^{1/2}$) of graphene is closer to DCM (20.3 MPa$^{1/2}$) than NMP (22.9 MPa$^{1/2}$). Another reason for the excellent dispersion stability of graphene in DCM might be that the density of DCM (1.33 g/cm^3) is relatively higher compared to NMP (1.03 g/cm^3). In fact, the gravimetric measurement of the concentration of graphene in dispersions was higher in NMP (1.3 mg/mL) than in DCM (0.7 mg/mL). The dispersion stability in ethanol (Δδ = 5.5 MPa$^{1/2}$ with graphene) was the most unstable and followed by THF.

In the presence of PVK-*b*-PVP, the dispersion stability of graphene can be listed in the following order: DCM > ethanol > THF > NMP. Figure 5(b) clearly indicates that the addition of PVK-*b*-PVP does not improve the stability of graphene dispersion confirms from the high TSI value which might be attributed to close similarities in both surface tension and solubility parameter between NMP and graphene. For ethanol and THF, the dispersions stability was extraordinarily improved and showed lower TSI values, as compared with pristine graphene dispersions in Figure 5(a).

Figure 6 shows the photographic images of graphene dispersions with the same time interval as that TSI analyses. Owing to the poor transmittance of graphene dispersions, sedimentation or phase separation is not clearly distinguished, but the stability of the dispersion can be roughly estimated with the photographs. The graphene dispersions with PVK and PVP are not stable in ethanol and THF but the dispersion with PVP in NMP is stable, these stable and unstable dispersions are attributed due to the solubility differences of the polymers in NMP, THF, ethanol, and DCM which are explained in the above sections. PVK-*b*-PVP forms micelles in both ethanol and THF and thus dispersing graphene quite well due to its amphiphilic nature. Mainly, PVK-*b*-PVP disperses graphene very well in ethanol, which is the most non-toxic and cost-effective among the solvents.

4. Conclusion

PVK homopolymer, PVP homopolymer, and PVK-*b*-PVP block copolymer were synthesized by RAFT polymerization, and these polymers were introduced to

prepare non-aqueous graphene dispersions with four different solvents, ethanol, NMP, DCM, and THF. Time-dependent TSI values from the graphene dispersions were correlated with solubility parameter and surface tension of solvents, polymers, and graphene. Our approach found that DCM would be a good candidate for pristine graphene dispersion like NMP. Both THF and ethanol can be good solvents for PVK-*b*-PVP to disperse graphene. Therefore, a systematic study for the effects of various polymers and solvents on the dispersion stability of graphene will be a great help to discover non-toxic, cost-effective, and recyclable solvents for single- or few-layer graphenes.

Acknowledgement

This work was supported by the Ministry of Trade, Industry and Energy, Korea (Grants No. 10044338, 10070241, and 10067082).

References

1. C. Lee, X.D. Wei, J.W. Kysar, J. Hone, *Science,* **321**, 385−388 (2008).
2. K.S. Novoselov, A.K. Geim, S.V. Morozov, D. Jiang, Y. Zhang, S.V. Dubonos, I.V. Girgorieva, A.A. Firsov, *Science*, **306**, 666−669 (2004).
3. K.I. Bolotin, K.J. Sikes, Z. Jiang, M. Klima, G. Fudenberg, J. Hone, P. Kim, H.L. Stormer, *Solid State Commun.*, **146**, 351−355 (2008).
4. M.J. Allen, V.C. Tung, R.B. Kaner, *Chem. Rev.*, **110**, 132−145 (2010).
5. X. Liang, Z. Fu, S.Y. Chou, *Nano Lett,.* **7**, 3840−3844 (2007).
6. D. Gunlycke, D.A. Areshkin, J. Li, J.W. Mintmire, C.T. White, *Nano Lett.*, **7**, 3608−3611 (2007).
7. A. Yu, I. Roes, A. Davies, Z. Chen, *Appl. Phys. Lett.*, **96**, 253105−253105 (2010).
8. P.K. Ang, W. Chen, A.T.S. Wee, K.P. Loh, *J. Am. Chem. Soc.*, **130**, 14392−14393 (2008).
9. C. Ataca, E. Aktürk, S. Ciraci, H. Ustunel, *Appl. Phys. Lett.*, **93**, 043123−043123 (2008).
10. C. Chung, Y.K. Kim, D. Shin, S.R. Ryoo, B.H. Hong, D.H. Min, *Chem. Res.*, **46**, 2211−2224 (2013).
11. G. Gu, S. Nie, R.M. Feenstra, R.P. Devaty, W.J. Choyke, W.K. Chan, M.G. Kane, *Appl. Phys. Lett.*, **90**, 253507−253507 (2007).
12. A. Reina, X. Jia, J. Ho, D. Nezich, H. Son, V. Bulovic, M.S. Dresselhaus, J. Kong, *Nano Lett.*, **9**, 30−35 (2009).
13. A. Ciesielskia, P. Samorì, *Chem. Soc. Rev.*, **43**, 381−398 (2014).
14. D. Nuvoli, L. Valentini, V. Alzari, S. Scognamillo, S.B. Bon, M. Piccinini, J. Illescas, A. Mariani, *J. Mater. Chem.*, **21**, 3428−3431 (2011).
15. J.N. Coleman, *Adv. Funct. Mater.*, **19(23)**, 3680−3695 (2009).
16. Y. Hernandez, V. Nicolosi, M. Lotya, F.M. Blighe, Z. Sun, S. De, I.T. McGovern, B. Holland, M. Byrne, Y.K. Gun'Ko, J.J. Boland, P. Niraj, G. Duesberg, S. Krishnamurthy, R. Goodhue, J. Hutchison, V. Scardaci, A.C. Ferrari, J.N. Coleman, *Nat. Nanotechnol.*, **3**, 563−568 (2008).
17. Y. Hernandez, M. Lotya, D. Rickard, S.D. Bergin, J.N. Coleman, *Langmuir*, **26**, 3208−3213 (2010).
18. W. Qian, R. Hao, Y.L. Hou, Y. Tian, C.M. Shen, H.J. Gao, X.L. Liang, *Nano Res.*, **2**, 706−712 (2009).
19. X.Y. Zhang, A.C. Coleman, N. Katsonis, W.R. Browne, B.J.V. Wees, B.L. Feringa, *Chem. Commun.*, **46**, 7539−7541 (2010).
20. A. Schlierf, H. Yang, E. Gebremedhn, E. Treossi, L. Ortolani, L. Chen, A. Minoia, V. Morandi, P. Samori, C. Casiraghi, D. Beljonne, V. Palermo, *Nanoscale*, **5**, 4205−4216 (2013).
21. J.M. Englert, J. Rohrl, C.D. Schmidt, R. Graupner, M. Hundhausen, F. Hauke, A. Hirsch, *Adv. Mater.,* **21**, 4265−4269 (2009).
22. A.B. Bourlinos, V. Georgakilas, R. Zboril, T.A. Steriotis, A.K. Stubos, C. Trapalis, *Solid State Commun.,* **149**, 2172−2176 (2009).
23. S. Perumal, H.M. Lee, I.W. Cheong, *J. Colloid Interface Sci.*, **497**, 359−367 (2017).
24. S. Perumal, H.M. Lee, I.W. Cheong, *Carbon*, **107**, 74−76 (2016).
25. H.M. Lee, S. Perumal, I.W. Cheong, *Polymers*, **8**, 101−112 (2016).
26. S. Perumal, K.T. Park, H.M. Lee, I.W. Cheong, *J. Colloid Interface Sci.*, **464**, 25−35 (2016).
27. V. Georgakilas, J.N. Tiwari, K.C. Kemp, J.A. Perman, A.B. Bourlinos, K.S. Kim, R. Zboril, *Chem. Rev.*, **116**, 5464－5519 (2016).
28. D.W. Johnson, B.P. Dobson, K.S. Coleman, *Curr. Opin. Colloid Interface Sci.*, **20**, 367−382 (2015).
29. Q. Li, C. Gao, S. Li, F. Huo, W. Zhang, *Polym. Chem.*, **5**, 2961−2972 (2014).
30. A. Karali, G.E. Froudakis, P. Dais, F. Heatley, *Macromolecules*, **33**, 3180−3183 (2000).
31. H. Shin, B.G. Min, W. Jeong, C. Park, *Macromol. Rapid Commun.*, **26**, 1451−1457 (2005).
32. H.K. Cho, I.W. Cheong, J.M. Lee, J.H. Kim, *Korean J. Chem. Eng.*, **27**, 731−740 (2010).
33. Y.-W. Jung, J.-W. Park, I. Kim, C.-S. Ha, *J. Adhesion Interface*, **6**, 1−7 (2005).

34. M. P. Stevens, Polymer Chemistry: an introduction, Oxford University press, revised 3rd Edn., (1999).
35. Y. Yu, Z. Wu, L. He, B. Jiao, X. Hou, *Thin Solid Films*, **589**, 852−856 (2015).
36. S. O'Driscoll, G. Demirel, R.A. Farrell, T.G. Fitzgerald, C. O'Mahony, J.D. Holmes, M.A. Morris, *Polym. Adv. Technol*., **22**, 915−923 (2011).
37. C.M. Hansen, Hansen solubility parameter: a user's handbook, CRC press, revised 2nd Edn., (2007).
38. A.E.D. Rio-Castillo, C. Merino, E. Díez-Barra, E. Vázquez, *Nano Res.*, **7**, 963−972 (2014).